Bollettino di Geofisica Teorica ed Applicata Vol. 53, n. 4, pp. 581-600; December 2012
DOI 10.4430/bgta0067

Airborne electromagnetics for groundwater salinity mapping: case studies of coastal and inland salinisation from around the world

A. Viezzoli[1], T. Munday[2] and Y.L. Cooper[2]

[1] *Aarhus Geophysics, Aarhus, Denmark*
[2] *CSIRO, Kensington (Perth), Australia*

(Received: July 12, 2011; accepted: April 4, 2012)

ABSTRACT Groundwater salinisation is a serious problem affecting numerous areas of the world, both in coastal and interior regions. Airborne electromagnetics (AEM) is a very effective tool for mapping hydrogeology, and therefore for managing salinisation related issues at large scale. We present here a representative collection of case studies from areas around the world describing its potential. In Banda Aceh, the applied methodology proved that the shallow aquifers did not suffer any long term effect from the tsunami of 2004. In Yucatan, it mapped the network of caves of that remote coastal Karstic environment. Along the south Australian coast, it provided hydrogeological insight from areas of a National Park which were interdicted to boreholes. In Venice AEM was used to add a great amount of data from the bottom of the lagoon, and to better understand the surface water-ground water interaction, in an area where geophysical measurements are particularly challenging, and borehole very sparse and, potentially, dangerous. Along the Murray Darling corridor, in south Australia, the technique was crucial in refining the understanding of dry land salinisation processes, and in trying to manage it. In the Okawango delta, it helped studying the surface water groundwater interactions, and the processes that keep the latter fresh while salt islands grow.

Key word: Airborne electromagnetics, salinisation, groundwater, hydrogeology, management.

1. Introduction

There are few places in the world where salinisation is not cause of major threat to groundwater resources. Sea water costal salinisation affects large portions of coastlines, and dry land (or inland) salinisation linked to evapotranspiration, or to raising of ancient brines affects many semiarid areas. These phenomena require proper management of groundwater, and of the interaction between groundwater, surface water, and the biosphere. The amount and detail of information required for managing these systems obviously varies in different settings, locations, and different level of human activities. Large scale models are however most often needed for the task. Geophysics is being used in some countries to obtain, relatively fast and cheaply, high density of data which relate to different physical parameters, and that can, integrated with ancillary information, produce very detailed groundwater models. Airborne Electromagnetics (AEM) is among the most widely used geophysical methodology for this purpose. Thanks to its

extreme speed of acquisition, lack of logistical problems linked to gaining access to the sites, and very low price surface area unit, it has become a crucial tool in countries like Australia, Denmark, Germany, United States, Canada (e.g., Siemon *et al*., 2004; Thomsen *et al*., 2004; Baldridge *et al*., 2007; Munday and Fitzpatrick, 2008; Moller *et al*., 2009; Viezzoli *et al*., 2009; Wiederhold *et al*., 2009).

In this paper we simply present a series of international case studies revolving around salinisation. In the Yucatan peninsula, the Venice lagoon, Banda Aceh and southern Australia, we will focus on sea water intrusion, whereas in the Murray Darling river basin (Australia) and the Okawango Delta (Botswana), on inland salinisation. The diversity of the studies presented, and also of the AEM systems used, give a representative sample of the methodology applied to groundwater mapping and management. However, we refer the interested reader that wants to get more into details of the technology, to several excellent reviews and technical papers on AEM theory (e.g., Fountain, 1998) data acquisition with different systems (e.g., Sorensen and Auken, 2004; Smith *et al*., 2009) , data processing and inversion (e.g., Brodie and Sambridge, 2006; Ley-Cooper *et al*., 2010), resolution (e.g., Beamish, 2003; Reid *et al*., 2006), depth of investigation (Peltoniemi, 1998; Christiansen and Auken, 2010) and systems comparisons (e.g., Liu and Asten, 1992; Siemon *et al*., 2009).

2. The methodology

AEM has been used now with success for more than a decade for mapping groundwater quality, i.e., groundwater salinity. The technique is mostly based on the Time domain EM (TDEM, or TEM), even though there are also frequency domain EM (FDEM, sometimes also referred to as HEM) systems. In both cases a time varying current pulsed in the Tx loop towed in the air induces a current in the ground. The response of the ground is then measured by the Rx coil, also airborne. The measured fields (time decaying voltage in TDEM, amplitude and phase shift in FDEM) contain information about the electrical resistivity of the ground. By deconvolving the measured response from the response of the AEM system (inversion), one can then recover the 3D resistivity voxel of the subsurface. See Siemon *et al*. (2009) for an overview of helicopter-borne systems present at the time.

Allowing large scale mapping, at high lateral and vertical resolution, down to considerable depths, AEM is often the tool of choice for the base study for salinisation related problems, to which other data types, e.g., direct measurements of lithological or EC variations are integrated. In this paper we present a range of case studies from different areas and applications around the world and different AEM systems, each one with a different peculiarity. We just present some key technical figures here: the depth of investigation is often in excess of 200 m for time domain systems, and of 100 m for frequency domain systems, the lateral resolution is in the order of several tens of metres, the vertical resolution from metres to tens of metres. We refer once more to other more technical papers (e.g., Macnae *et al*., 1998; Sengpiel and Siemon, 2000; Brodie and Sambridge, 2006; Siemon, 2006; Huang and Rudd, 2008; Viezzoli *et al*., 2008) for an in depth discussion of the different methodological aspects revolving around AEM, from data acquisition to modeling. It is however necessary to mention here that hydrogeological applications are not "bump finding" or "anomaly picking" exercises. The quantitative results demanded from AEM

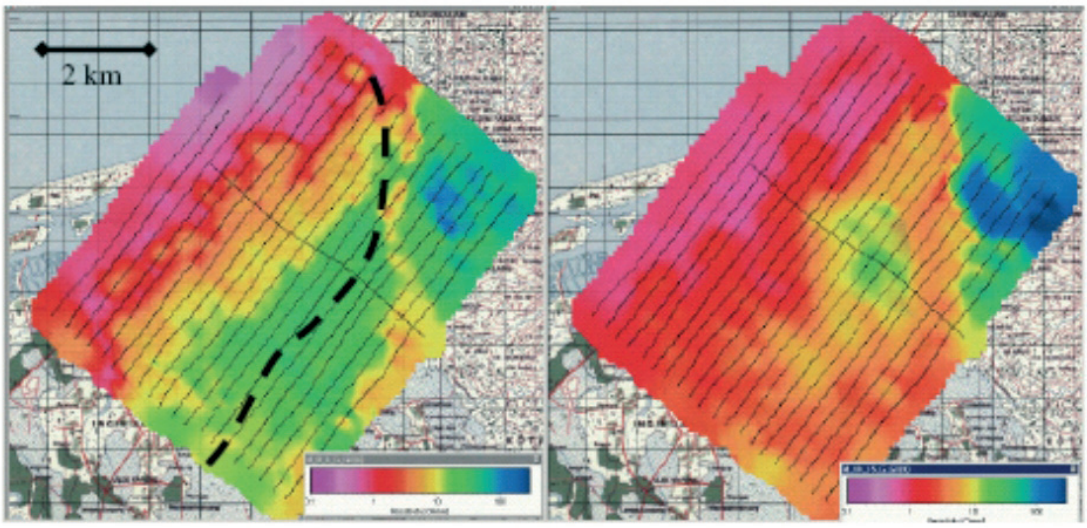

Fig. 1 - Average resistivity maps at 5-10 (left) and 15-20 m (right) depth intervals. The dashed line represents the approximate extent of the tsunami waves. Flight lines are represented by thin black lines.

for hydrogeological applications can only be achieved by means of good data quality, proper and transparent data processing, accurate full data inversion, and proper integration with ancillary information.

3. Sea water intrusion

3.1. Banda Aceh

Few months after the Boxing Day tsunami that hit south-eastern Asia in 2004, an AEM survey (BGR Dighem system) was carried out to asses weather the near surface aquifers had been affected. This survey was carried out with a helicopter-borne frequency domain (HEM) system by BGR, with five different frequencies and different transmitter-receiver separations, according to the parameters shown in Table 1. Tx and Rx coils are housed in a cylindrical "bird", towed behind the helicopter. The nominal altitude of the EM sensor is at 30-40 m above ground level, but it is continuously monitored by a laser altimeter. Exploration depth was of about 100 m (Siemon *et al*., 2007).

Fig. 1 shows the average resistivity map at 5-10 m (left) and 15-20 m (right) depth below surface. It is possible to evaluate a good agreement between the more conductive area (less than 1 ohm·m) and the extent of the tsunami waves, marked by the black dashed line. However, the

Table 1 - HEM system parameters for the Banda Aceh survey of 2004 by BGR.

System frequency (Hz)	387.2	1820	8225	41550	133200
Tx-Rx separation (m)	7.94	7.93	7.93	7.91	7.92

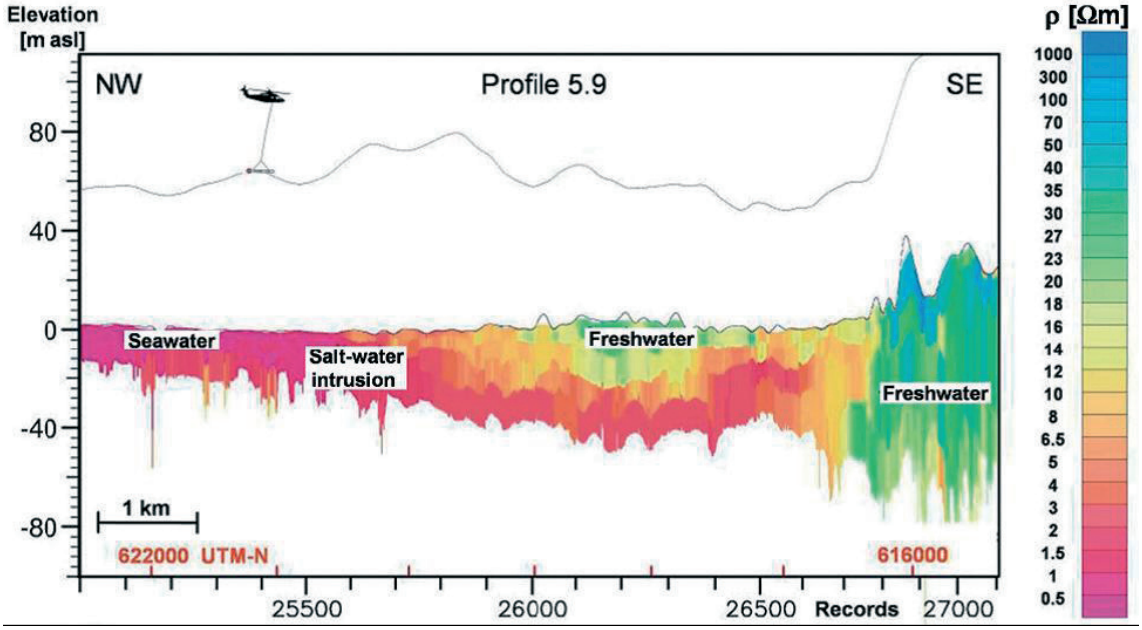

Fig. 2 - Vertical resistivity section of profile running from the sea to inland (adapted from Siemon *et al.*, 2007).

tsunami did not have a permanent effect on the near surface aquifers, since the highest conductivity values remain confined along the coastline. On the contrary, it is clear the seawater intrusion inland from the canals and rivers, as such as the deeper aquifers do show saline contamination, which is not correlated with the tsunami event.

The vertical resistivity section shown on Fig. 2, which runs from the sea to inland, is able to image better the deepening of the sea-water/fresh-water interface. A lens of freshwater floats above the sea-water and it is marked by resistivity of 20-30 ohm·m.

Conductivity, hence salinity, of groundwater decreases greatly at large distance from the coastline (more than 6 km), where volcanics prevail. Here resistivity reaches values larger than 100 ohm·m. Thanks to the electromagnetic survey several potential freshwater occurrences were found and mapped. These areas of higher resistivity (usually more than 20 ohm·m) have been selected for drilling new shallow wells. The prospection was useful also to locate sites for sanitary landfills, showing the lowest degree of environmental hazard.

See Siemon *et al*. (2007) for a more detailed description of the project.

3.2. Yucatan, seawater intrusion along Karstic coastline

The Sian Ka'an Biosphere is found on one of the world's largest and most striking Karst aquifers, located in the Yucatan peninsula in Mexico. Most of the fresh water supplied to the thick jungle and wetlands in Sian Ka'an comes from the groundwater aquifer; it is stored in submerged caves and underground rivers which have carved their way through the fractured limestone host rock matrix.

Water scarcity and quality is a problem prevailing in the Yucatan peninsula region, mainly

Table 2 - Austrian HEM system parameters.

System frequency (Hz)	340	3200	7190	28850
Tx-Rx separation (m)	4.53	4.53	4.49	4.66

because of the moving demographic dynamics and poor governance on the soaring tourism industry demands. This has left Sian Ka'an in a vulnerable situation. Ensuring there is enough water for both the wetlands and human use has attracted much attention posing and interesting challenge to groundwater management. Gondwe (2010) dissertation is a document developed "with the ultimate aim of improving the management of the groundwater resources".

A multi frequency helicopter electromagnetic survey was carried towards the north of Sian Ka'an, in Yucatan Mexico (Supper *et al*., 2009). The parameters of this system (Austrian airborne) are reported on Table 2. In this case four frequencies were adopted, with a sensor altitude of about 40 m; also in this case a laser altimeter provided the correct altitude values during the flight. According to Supper *et al*. (2009) the lowest frequency allowed to reach a penetration depth of about 120 m, but it must be considered that it is strongly dependent on the mean underground resistivity, so these values must refer to the areas with no seawater intrusion.

This survey aimed at providing insight into the hydrogeology of the area, in particular about the network of underground caves and sinkholes (the "Cenotes"), some connected to the open sea and affected by seawater intrusion. Results of gridded channels and their in-phase two frequency inversion were presented in Supper *et al*. (2009), which show that the contrasts in conductivities are enough to be detected and can be mapped.

Other cases of successfully mapping Karst structures have been presented in the past (Beard *et al*., 1994). In order to quantitatively asses the results, the water quality and determine the possible depths of the caves and tunnels, we processed and calibrated the data (see Ley-Cooper and Macnae, 2007). Fig. 3 has been presented in Gondwe (2010); it shows most structures can be correlated with the location of sink-holes known from cave maps constructed by scuba divers. Some of these structures had not previously been mapped by divers but some others structures have been verified with dive expeditions following the AEM campaign.

The image shows an interesting network of Karstic tunnels, which have formed at different geological stages i.e., at different depths, resulting in a halocline mix. The AEM has been gridded to show the fresh water from the inland as cold colours and poorer water quality as warm colours. A salt water intrusion is also present in this aquifer, and can be seen as it pushes its way from the east past the coastline boundary (brown line) and tends to migrate through preferential paths using the existing tunnels which are known to connect at sea at different locations and depths.

The delineation of Karstic caves mapped using the AEM are shown as prominent green linear features which have been overlaid by black dendritic cave map paths produced by scuba divers, to show the close correlation between the independent data sets.

3.3. South Australia

This case study presents a more typical example of seawater intrusion, from Coffin Bay, in south Australia. The area investigated is part of a national park, where no drilling could be done,

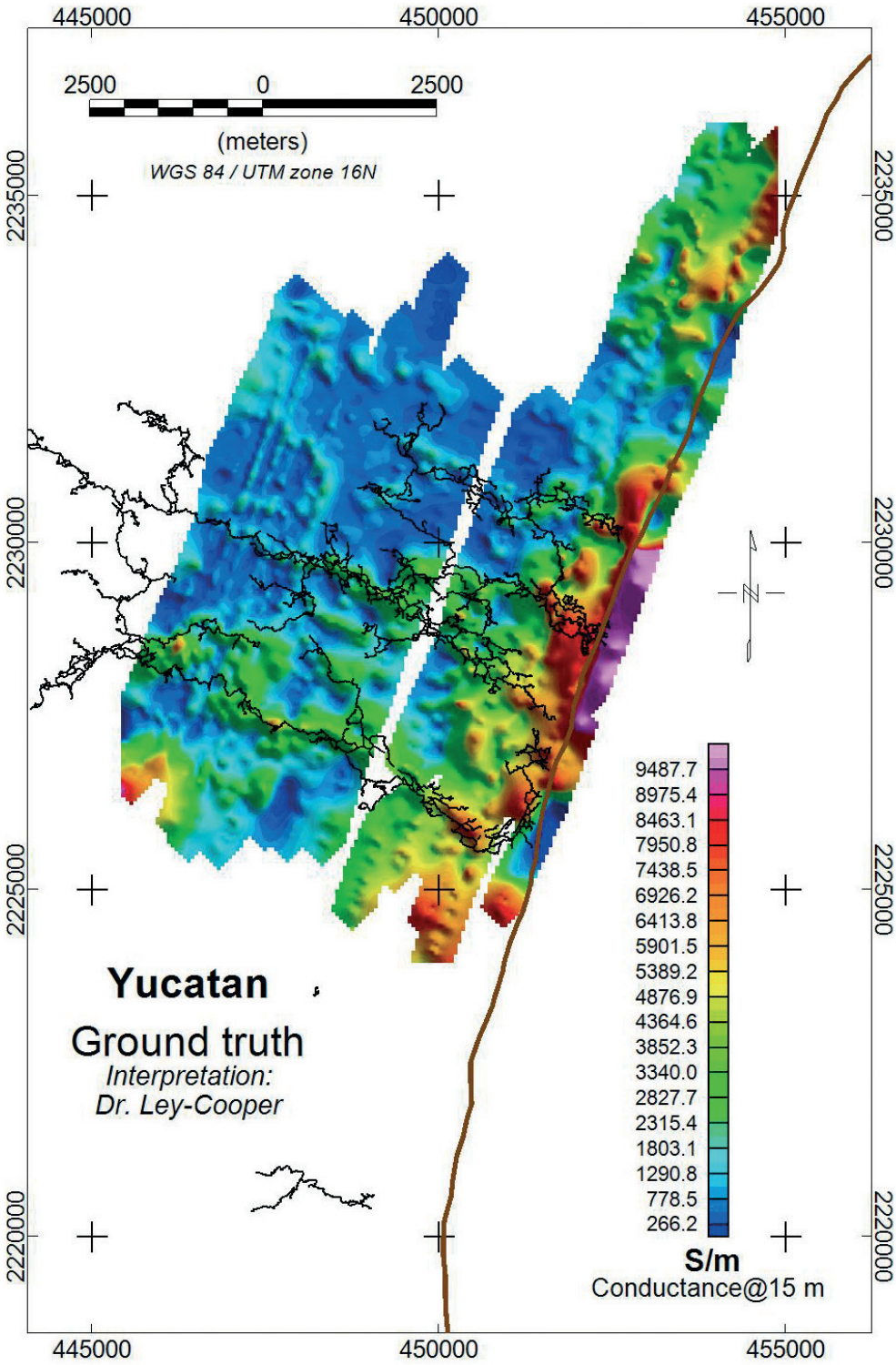

Fig. 3 - AEM conductivity map at 15 m depth, overlaid by speleological cave routs mapped by cave divers (black dendritic pattern). Brown line to the east of the map delimits the coast line.

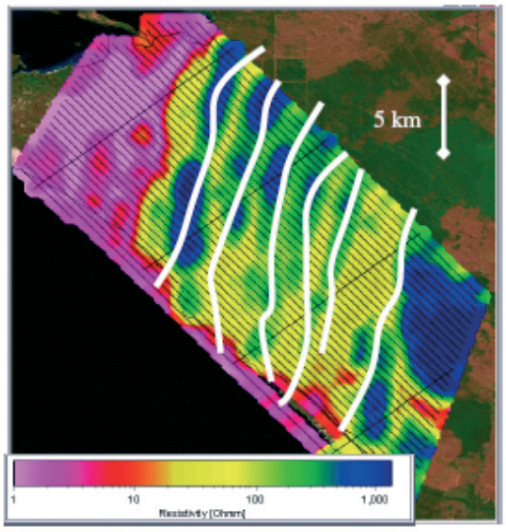

Fig. 4 - Resistivity map at 60-80 m depth, with location of magnetic maxima superimposed (white lines).

so that AEM was the only chance to gather the required information for the management of the shallow fresh water lenses, and the deeper groundwater resources, upon which the development of the area depends.

The system adopted was a fixed-wing time-domain one, TEMPEST [see Lane *et al*. (2000) for a detailed system description]. It used a base frequency of 25 Hz, with a square waveform and a 50% duty cycle (that is equal on and off times). Peak current was 300 A, so that the peak moment was 55800 A·m^2. The nominal altitude of the EM receiver is at 70 m above the ground level, while the transmitter is located on the aircraft flying 50 m higher and 100 m ahead. Navigation data are obviously monitored to make the necessary corrections. The sensor uses 3 perpendicular dB/dt coils, so to acquire both vertical and horizontal components of the secondary magnetic field. Voltage decay is sampled by 15 time gates, spanning from 0.013 ms to 16.2 ms. The large moment and the relatively long acquisition time allow to explore great depths, within hundreds of metres; of course, also in this case, the vertical resistivity distribution can influence greatly the effective penetration depth, so that to limit strongly it, in presence of conductive layers.

In Fig. 4 the progression of seawater intrusion across the entire coastal area, is evident. This resistivity map is related to a depth of 60-80 m. Very low resistivity values (less than 1 ohm·m) prevail along all the coastline, but it is quite clear a stronger encroachment on the NW side, due to the presence of the sea surrounding the peninsula. This means that the contamination of the coastal aquifers is really enhanced and it involves deep structures. Many high resistivity (up to 1000 ohm·m) lenses show an alignment roughly from north to south. The white lines show the location of positive magnetic anomalies, which are coincident with resistivity maxima. We can interpret these units as the uplift of the basement. Fig. 5 shows a vertical resistivity section, running from SW to NE. It is clear the huge sea-water intrusion, with the interface with the fresh-water resting at about –50 m a.s.l. At the right side of the section, the resistive and magnetic basement is well imaged.

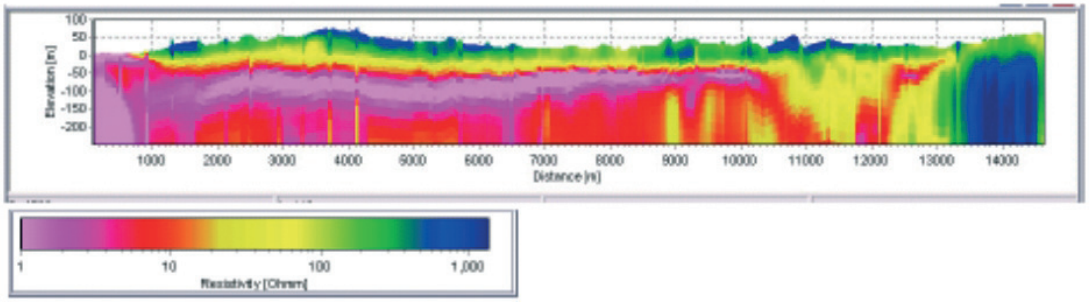

Fig. 5 - Vertical resistivity section, for the northernmost tie line in Fig. 4. Seawater intrusion in pink, resistive basement on the right hand side in blue. Same colorscale as Fig. 4.

The information provided by AEM allows a much more comprehensive understanding of the hydrogeology of the area, filling in the gaps due to lack of boreholes data within the national park. See for example Fig. 6, reporting a comparison between borehole-derived and AEM-derived elevation of the base of the Quaternary limestone layer. On these bases the shallow aquifers of the area will be managed more effectively.

3.4. Venice

The SkyTEM survey conducted in the Venice lagoon, Italy [see Viezzoli *et al*. (2010) for detailed results] allowed to significantly improve the knowledge about the lagoon and nearby

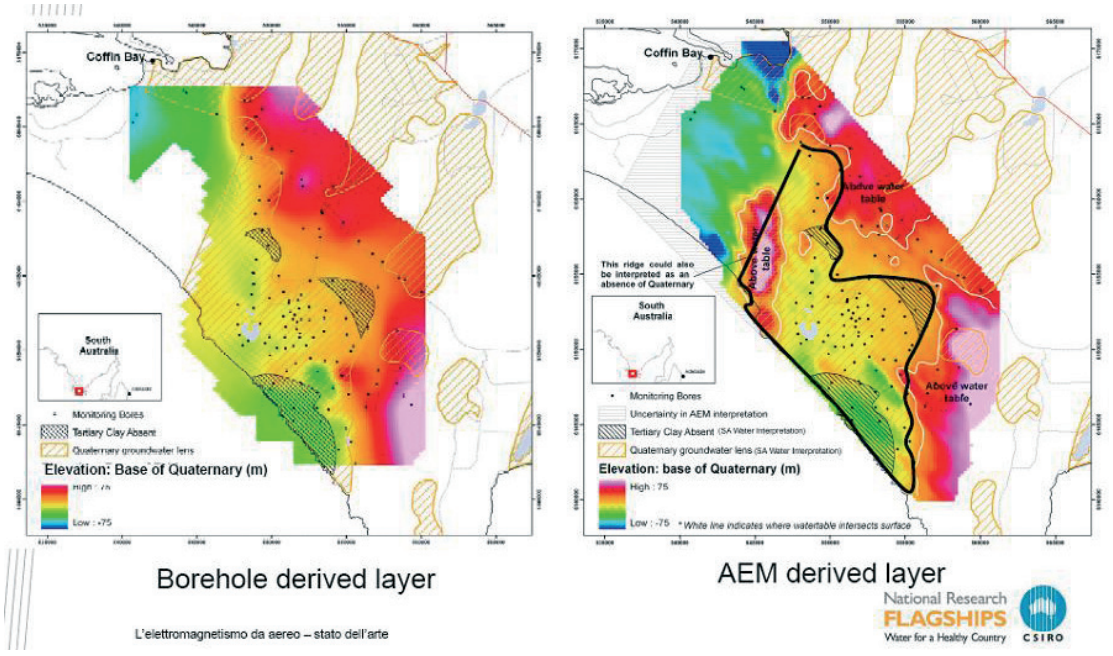

Fig. 6 - Borehole derived (left) and AEM derived elevation of base of Quaternary limestone in the area.

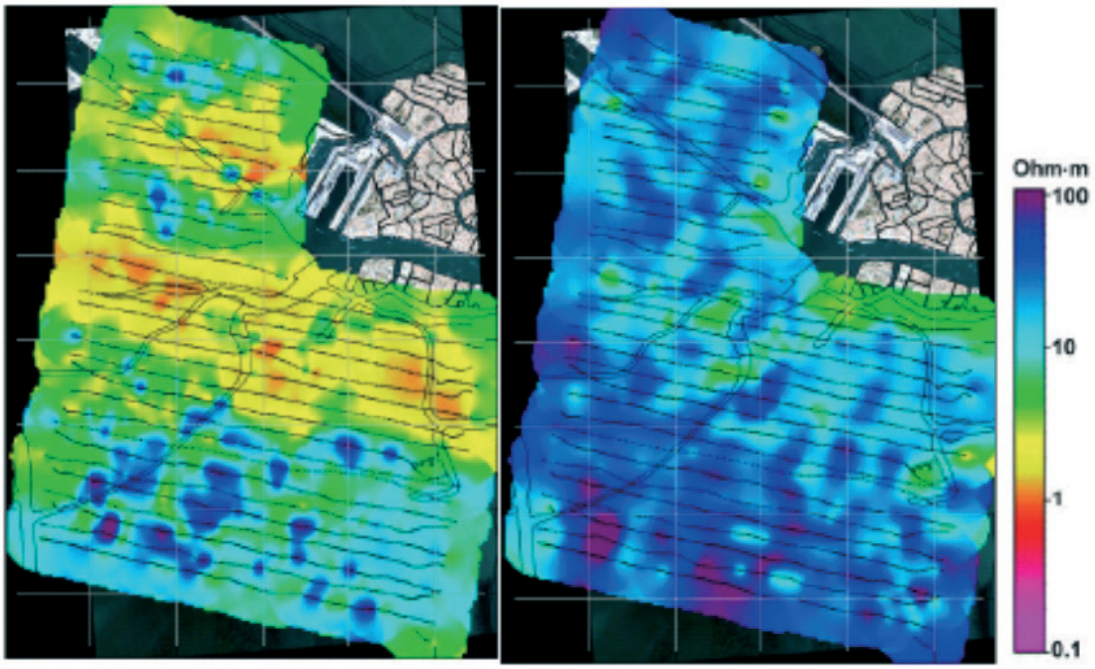

Fig. 7 - Central Venice lagoon: resistivity map at 20-30 m depth (left) and 40-60 m depth (right).

coastland subsurface. The environment was very challenging, as it consists of salt marshes, mud flats, shallows, tidal channels, islands, together with reclaimed farmlands crossed by natural watercourses and drainage channel networks. SkyTEM [see Sorensen and Auken (2004) for a detailed description] is a helicopter time-domain AEM system. In this survey, it used a transmitter having an area up to 492 m^2 and peak current of more than 100 A. The receiver unit is set just above the transmitting loop, simulating a quasi-central mode. Thanks to differential use of a single turn array or of a four turns array, and to different levels of energization, the system is able to operate by two different set-up: a Low Moment and a High Moment. It is possible therefore to collect data both from very shallow and deeper targets (up to 200-300 m below ground level), by assuring however a good vertical resolution. This is possible also by means of the great range of the time gates, spanning from 10-12 μs to 7 ms from beginning of ramp down. Navigation data (altitude, tilt, position) are continuously monitored. Nominal altitude of the Tx-Rx frame is at 30 m above ground level.

The AEM prospect has shown the presence of fresh water (with resistivity larger than 20 ohm·m) underneath the central part of the lagoon (close to Venice city), at shallow depth also, i.e., from 20 to 30 m (Fig. 7, left). At the same depth, two main paleochannels, filled with fine materials (clays and silts) were resolved thanks to their low resistivity (1-2 ohm·m). Going into depth, at 40-60 m (Fig. 7, right), the freshwater aquifers are more evident, reaching resistivity up to 100 ohm·m.

Moreover, the source and inland extent of the saltwater contamination in the shallow coastal aquifers, along the southern margin of the lagoon (near Chioggia town) have been clearly

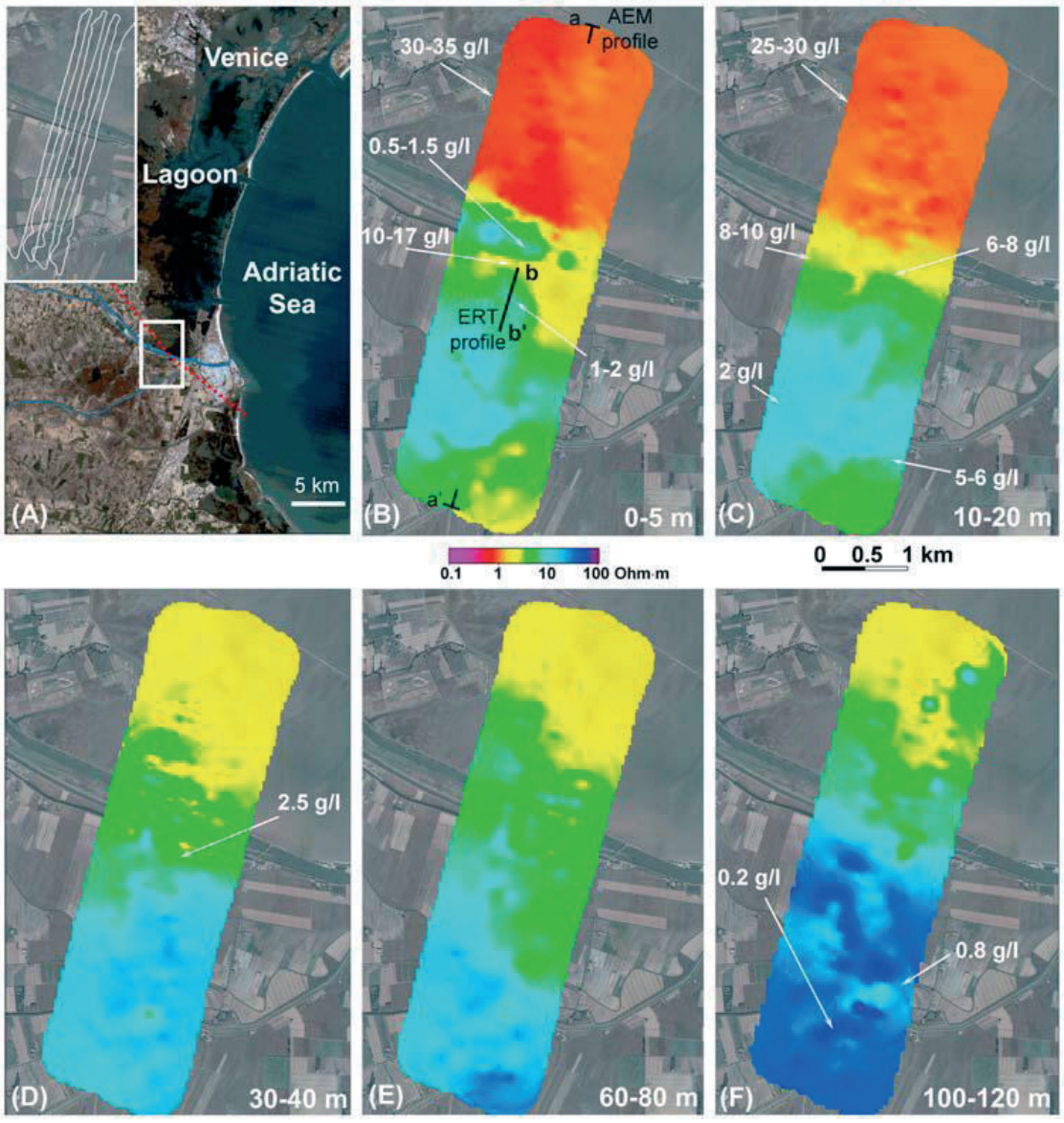

Fig. 8 - Resistivity maps at different depths. A shows the survey area location. In B the vertical resistivity section is drawn (a-a'), b-b' is referred to an ERT profile (not discussed in this paper). Numeric values show salinity of water collected by samples.

highlighted. Fig. 8 shows a series of resistivity maps, extracted from depths ranging from the surface down to 120 m. The highly conductive response of the lagoon water (B), which is located in the northern side of the maps and of the bottom sediments (C) is sharp. It is clear the encroachment of the salt-water southwards, i.e., inland, as confirmed by salinity values of collected water samples. In B is clear the local effect of a stream that causes a partial increase of resistivity, as confirmed by salinity values of 0.5-1.5 g/l.

At 30-40 m (D) the resistive fresh-water aquifers are more clearly imaged, on the inland side,

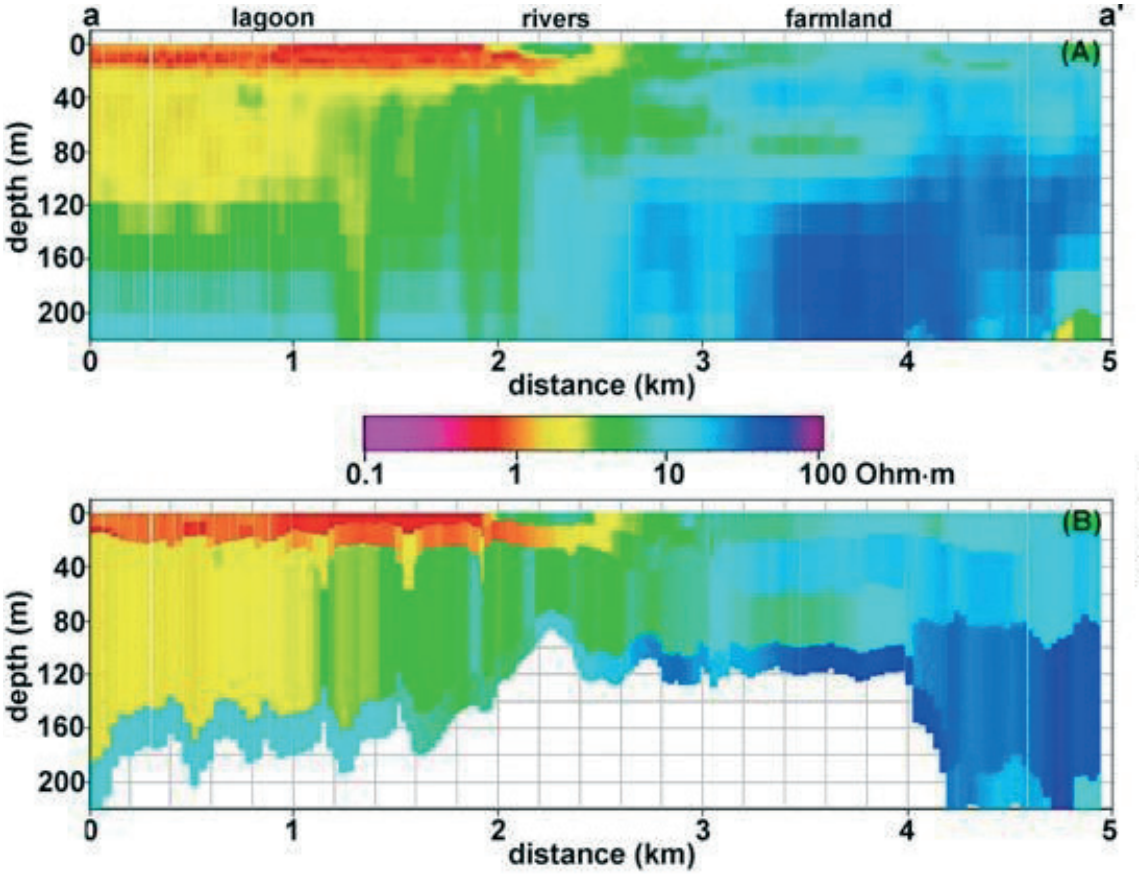

Fig. 9 - Vertical resistivity section (a-a' in Fig. 7B), running from north to south. The upper section shows the result of a multi-layered inversion, while below it is shown the few-layered one.

so that at great depths (F), between 100-120 m, the resistivity values higher than 50 ohm·m are connected to very low salinity (0.2-0.8 g/l).

Fig. 9 shows the vertical resistivity section, drawn on B as a-a'. It shows more clearly the lagoon water ingression (marked by the red-yellow colours) and the deep fresh aquifers inland (blue layers). The exploration depth has been estimated within 200 m. A sharp contact within the lagoon sediments is clearly visible from the section at a depth of about 120 m, marked by decreasing resistivity with depth: this may be the interface between different relevant stratigraphic units, e.g., the clayey layer bounding the Holocene-Pleistocene sedimentation.

4. In land salinisation

4.1. South Australia

South-eastern Australia suffers from ongoing dry land salinisation problems due to ancient salt stores being remobilized by lifting groundwater table. Even though this is largely a natural

phenomenon, human activities, such as excessive irrigation, have aggravated it. A sound understanding of the spatial variability of the hydrogeology is demanded for proper management of these areas, and its possible remediation. In this case we present results from the area of Bookpurnong, in south Australia, were a number of subsequent AEM surveys have been conducted over the last 5 years, in order to monitor the near surface variability of the hydrogeological systems.

The Bookpurnong floodplain, located approximately 12 km upstream from the township of Loxton in the lower Murray region of south Australia has been the focus of trials to manage a marked decline in tree health that has been observed along the River Murray in south Australia and elsewhere. The primary cause for this decline is recognised as a combination of floodplain salinisation from saline groundwater discharge, the decrease in flooding frequency, and the recent drought.

The study area has a hydrogeology characteristic of the eastern part of the lower Murray River and is represented schematically in Fig. 10.

Floodplain sediments consist of a clay (the Coonambidgal Clay), overlying a sand (the Monoman Formation). These sediments occupy the Murray Trench which cuts into a sequence of Pliocene sands (the Loxton-Parilla Sands). These sands outcrop in the adjacent cliffs, and are covered by a layer of Woorinen Sands over Blanchetown Clay. The whole area is underlain by the Bookpurnong Beds, which act as an aquitard basement to the shallow aquifer that encompasses the Monoman Formation and Loxton Sands. High recharge from irrigation on the highlands adjacent to the floodplain results in the development of localised perching and the formation of a groundwater mound in the Loxton-Parilla sands. The mound increases the hydraulic gradient towards the floodplain causing a rise in water levels in the floodplain sediments. Groundwater seepage at the break of slope adjacent to the cliffs may also occur. High water levels coupled with high rates of evapotranspiration, concentrates salt in the near surface across the floodplain. Elevated groundwater levels in the floodplain also promote the discharge of saline groundwater into the Murray River, along what are termed “gaining” stretches of the river system. Elsewhere along the river, river water discharges into the adjacent banks and we have extensive reaches that are referred to as “losing” stretches.

Fig. 11 shows, with a cross section from inversion results of a SkyTEM survey, the mechanism taking place. Notice the correlation between near surface resistivity (directly connected to groundwater salinity) and areas of vegetation loss in the floodplains, and of healthy vegetation close to the Murray River, which, locally, recharges the shallow groundwater. Numbers superimposed to the sections show the EC from boreholes in the area. Their spatial variability well matches the one of the electrical resistivity obtained from the AEM.

Fig. 12 shows the variation in near surface conductivity in the area, as obtained from inversion of two different AEM datasets (RESOLVE and SkyTEM) acquired over 3 years. The RESOLVE system (by Fugro) is a multi-frequency helicopter-borne one and its parameters are reported in Table 3 (see Cain, 2003 for more details).

The receiver coil orientation is coplanar, except for the 3300 Hz, that is coaxial. The EM sensor flies at a nominal altitude of 30 m. Both in-quadrature and in-phase components of the secondary field are acquired. Even though issues of cross calibration between the data sets

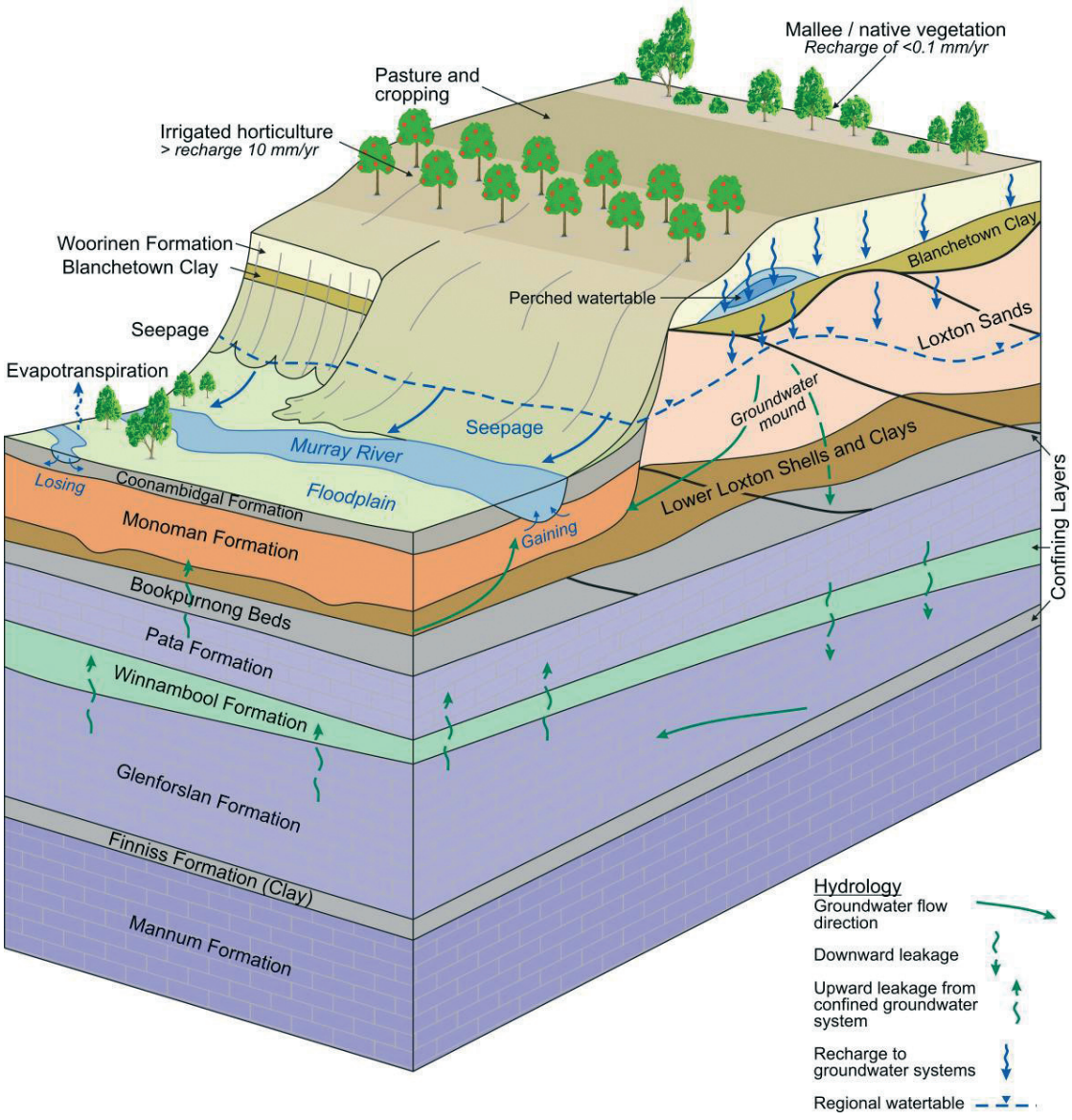

Fig. 10 - Schematic representation of the hydrogeology of the Bookpurnong floodplain and adjacent highland areas.

complicate this exercise, it seems that AEM can also be used effectively as a tool for time lapse monitoring of groundwater salinity in these dynamic environments.

Black arrows indicate stretches of the river which gain salinity from discharging

Table 3 - Resolve HEM nominal system parameters.

System frequency (Hz)	385	1800	3300	8200	40000	140000
Tx-Rx separation (m)	7.80	7.80	9.00	7.80	7.80	7.80

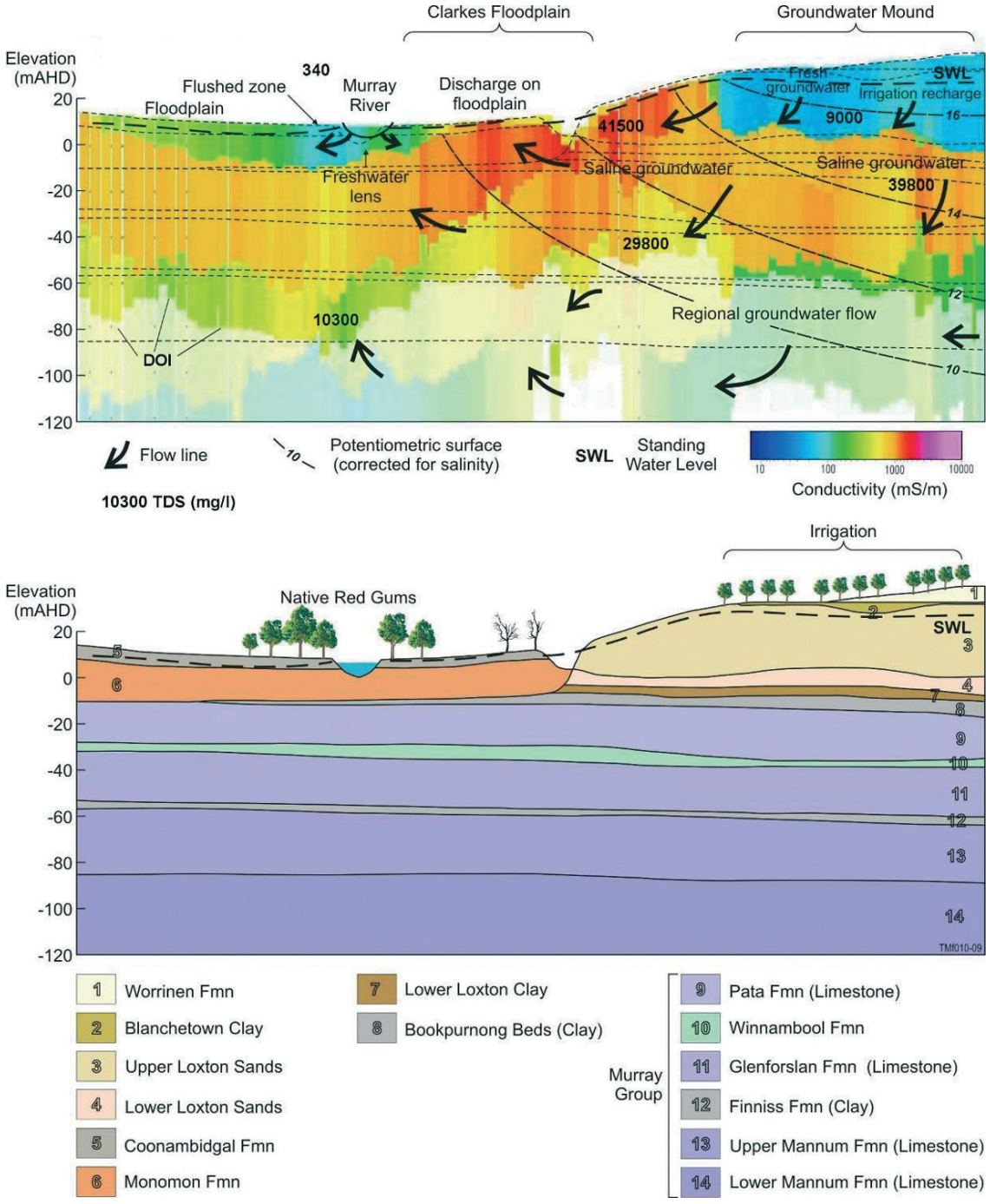

Fig. 11 - Vertical conductivity depth section derived from a 4 layer SCI of SkyTEM data for the floodplain – highland transect. The hydrogeology is illustrated in the lower section. Groundwater flow lines have been superimposed over the section and have been derived from an understanding of the potentiometric heads in the different aquifers. Groundwater conductivity values from bores in the vicinity of the section line 2 are projected onto the section for reference.

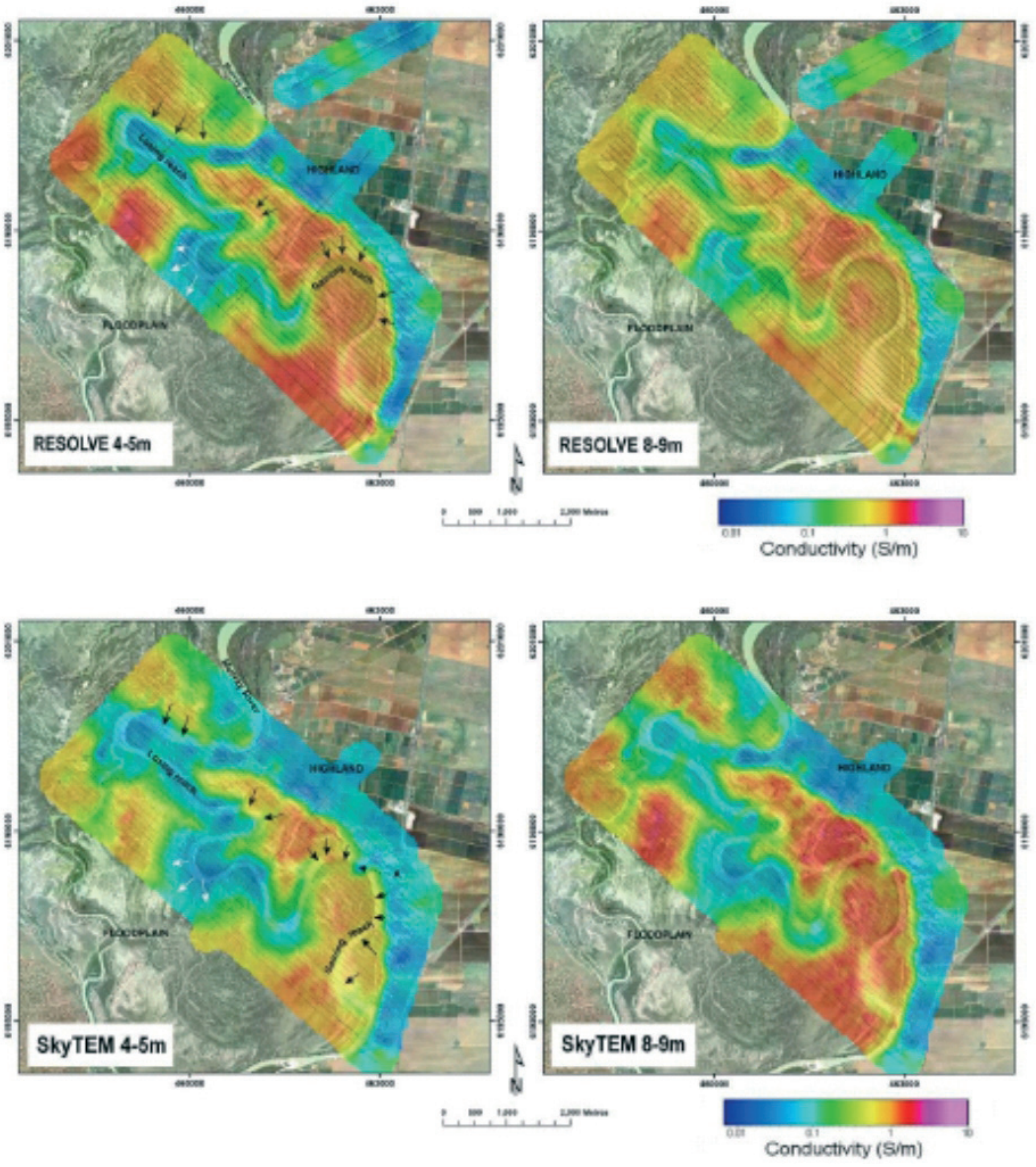

Fig. 12 - Interval conductivity images for the different depth intervals derived from SCI inversions of the RESOLVE (top) and SkyTEM (bottom) data sets covering the Bookpurnong floodplain.

groundwater, whereas white arrows indicate stretches which lose fresh water from the river into the adjacent floodplain. A wide flushed (resistive) zone is apparent along significant stretches of the river through this area. The resistive zone at locality 'A' (indicated by the dashed arrow on the 4-5 m interval conductivity) may represent a drawdown of fresh river water into the substrate through over pumping of salt interception bores on the adjacent floodplain.

4.2. Okawango Delta

The AEM prospection in Okavango Delta region (Botswana) had as objective the mapping of

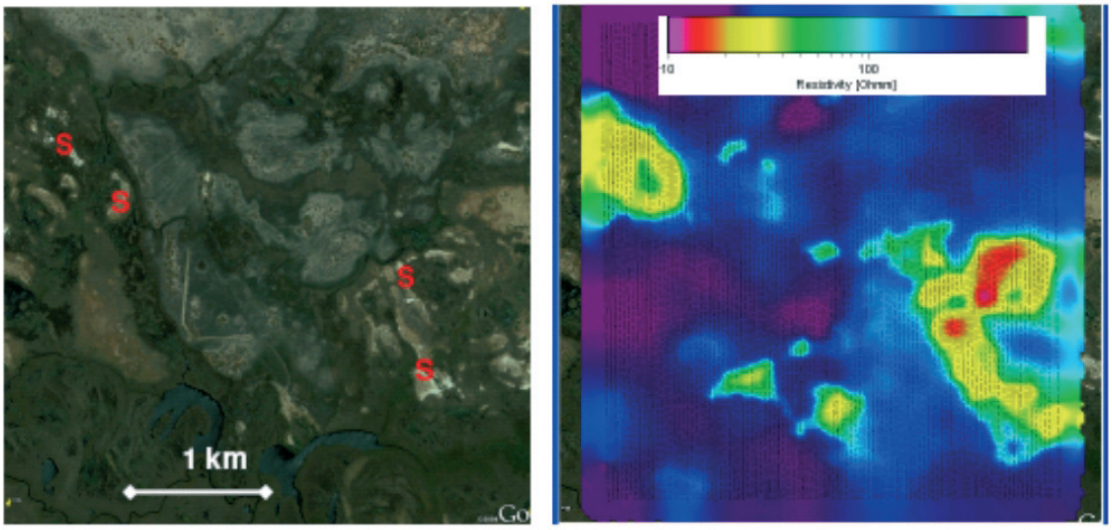

Fig. 13 - Satellite image of the survey area (left). Areas marked by "S" show the presence of surficial salt deposits. Resistivity map at 20-40 m depth (right). The areas with low resistivity (from yellow to red colours) are related to the downward salt plume into the islands.

freshwater-saltwater interface, the search for freshwater resources and the mapping of the regional geological setting. The AEM survey was performed by VTEM system (by Geotech), a time-domain helicopter-borne system [see Witherly *et al*. (2004) for more details]. The Tx loop has a dodecagon shape of 540 m^2, while the peak current is up to 310 A, so that the peak moment is up to 625000 NIA. Base frequency is usually 25 or 30 Hz, depending on AC power network frequency.

The sedimentary aquifer system consists of Kalahari sand beds with fluvial and lacustrine sediments, aeolian sands, silcretes and calcretes. Within the delta the unconfined sandy aquifers are composed of freshwater while the deeper aquifers are generally saline or brackish (5 g/l or more). The transition between fresh to barckish wateroccurs at depths of up to tens of metres. Moreover, there can be salinity plumes that complicate the hydrogeological setting.

According to MacCarthy (2006) the islands in the delta act like sinks for the salts transported by the river. Fig. 13 (left) shows a high resolution satellite picture of some of the islands in a portion of the survey area. Areas covered with salts are visible as white surfaces (marked by S). Fig. 13 (right) reports the average resistivity map at depth of 20-40 m, after data inversion: the conductive response located in the middle of the islands images the downward plume, density driven, of salty waters, that from the surface reach the deeper salty acquifers. For more details see Podgorski *et al*. (2010).

5. Discussion and conclusions

AEM is a tool perfectly suitable for mapping quantitatively the hydrogeology. Integrated with

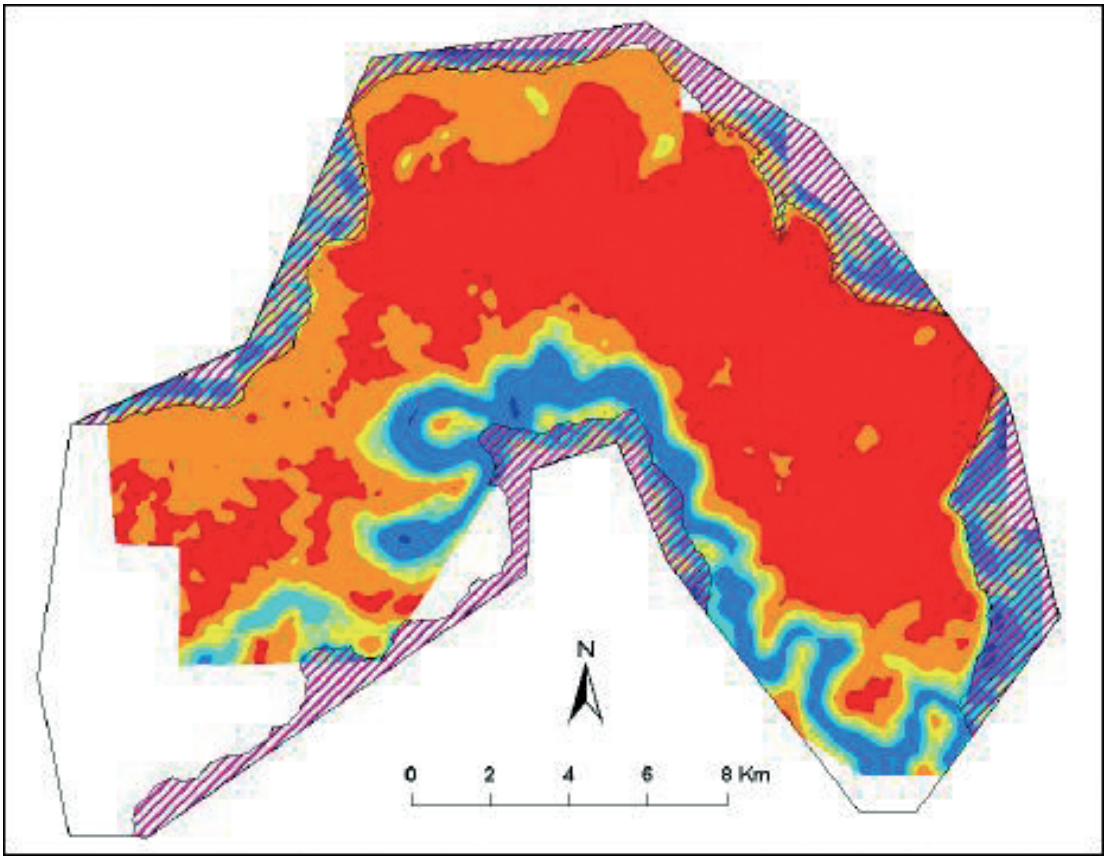

Fig. 14 - Salt store, as obtained integrating AEM and borehole information.

sparse ancillary information collected at the surface, or downhole, it represents a powerful tool for managing salinisation related issues, both along the coasts and inland, at large scale and high resolution.

Of course, each AEM system has its pros and cons, dictated by the technical features of the equipment, but a detailed review of the available systems is out of the scope of this paper. We will just mention that, in general, better vertical resolution and greater penetration depths is achieved with the time-domain systems, while the frequency-domain can be more suitable for shallow prospecting. Fixed-wing systems are usally more powerful and cheaper than helicopter systems, at cost of poorer lateral and near surface resolution, and adaptability to topographical variations.

In order to apply AEM as a tool for time lapse monitoring, great care needs to be taken in cross calibration of different data sets, acquired over time, with different AEM systems.

One of the main advantage of the method is the ability to investigate very large area (within many km^2) in a short time and with low costs, above all in comparison with any ground-based geophysical techniques. It must be underlined that this can be achieved without degrading the lateral and vertical resolution, and by warranting anyway a remarkable exploration depth (down to 200 m and more). AEM is also well suited for data integration, e.g., with seismic, satellite or borehole data.

The main limitations are a considerable start up cost, the presence of a minimum survey area below which it is not economically reasonable, the sensitivity to infrastructures, the lateral and vertical resolution which is lower than the one achievable, even though at greater cost, and much slower, with groundbased geophysics, e.g., geoelectrics at small electrode spacing.

The characteristics of the technique make it particularly appealing to build the basis of a solid management of salinisation realated issues, over large areas. This is to be integrated locally with ancillary data of higher resolution, for ground truething and "hydrogeological calibration", in order to obtain customised derived products that can be readily used by decision makers.

Fig. 14 shows an example of a possible derived product (the amount of salt stored in a given aquifer) obtained combining large scale AEM data with sparse borehole information (Munday and Fitzpatrick, 2008).

Acknowledgements. This paper was invited after, and is based upon an oral presentation delivered at GNGTS 2010, held in Prato.

REFERENCES

Baldridge W.S., Cole G.L., Robinson B.A. and Jiracek G.R.; 2007: *Application of time-domain airborne electromagnetic induction to hydrogeologic investigations on the Pajarito Plateau, New Mexico, USA.* Geophys., **72**, B31-B45.

Beamish D.; 2003: *Airborne EM footprints.* Geophys. Prospect., **51**, 49-60.

Beard L.P., Nyquist J.E. and Carpenter P.J.; 1994: *Detection of Karst structures using airborne EM and VLF.* In: Proc. 64th SEG Meeting, Los Angeles, CA, USA, expanded abstracts, pp. 555-558.

Brodie R. and Sambridge M.; 2006: *A holistic approach to inversion of frequency-domain airborne EM data.* Geophys., **71**, G301-G312.

Cain M.J.; 2003: *Survey report, helicopter-borne RESOLVE EM and magnetic geophysical survey.* U.S. Department of Energy, Powder River Basin coal bed methane demonstration survey, Mississauga, Ontario, Canada.

Christiansen A.V. and Auken E.; 2010: *A global measure for depth of investigation in EM and DC modeling.* In: Proc. 21st Int. Geophys. Conf., ASEG, Sydney, Australia, extended abstract, pp. 1-4.

Fountain D.; 1998: *Airborne electromagnetic systems – 50 years of development.* Explor. Geophys., **29**, 1-11.

Gondwe B.R.N.; 2010: *Exploration, modelling and management of groundwater-dependent ecosystems in Karst – the Sian Ka'an case study, Yucatan, Mexico.* PhD Thesis, DTU Environ., Depart. of Environ. Eng., Tech. University of Denmark, 87 pp.

Huang H. and Rudd J.; 2008: *Conductivity-depth imaging of helicopter-borne TEM data based on a pseudolayer half-space model.* Geophysics., **73**, F115-F120.

Lane R., Green A., Golding C., Owers M., Pik P., Plunkett C., Sattel D. and Thorn B.; 2000: *An example of 3D conductivity mapping using the TEMPEST airborne electromagnetic system.* Explor. Geophys., **31**, 162-172.

Ley-Cooper A.Y. and Macnae J.; 2007: *Amplitude and phase correction of helicopter EM data*. Geophysics, **72**, F119-F126.

Ley-Cooper A.Y., Macnae J. and Viezzoli A.; 2010: *Breaks in lithology: interpretation problems when handling 2D structures with a 1D approximation.* Geophysics, **75**, WA179-WA188.

Liu G. and Asten M.; 1992: *A comparison of airborne and ground transient EM systems in their resolving power against geological noise.* Explor. Geophys., **23**, 197-200.

MacCarthy T.S.; 2006: *Groundwater in the wetlands of the Okavango Delta, Botswana, and its contribution to the structure and function of the ecosystem.* Journal of Hydrogeology, **320**, 264-282.

Macnae J., King A., Stolz N., Osmakoff A. and Blaha A.; 1998: *Fast AEM data processing and inversion.* Explor. Geophys., **29**, 163-169.

Moller I., Sondergaard V.H., Jorgensen F., Auken E. and Christiansen A.V.; 2009: *Integrated management and utilization of*

hydrogeophyscal data on a national scale. Near Surf. Geophys., **7**, 647-659.

Munday T. and Fitzpatrick A.; 2008: *The targeted application of AEM for salinity mapping, interception and disposal: an illustration of the multifarious role of helicopter EM data in environmental management across the Murray Basin of Southeast Australia.* In: Proc. 5th Int. Conf. Airborne Electromagn., Haikko Manor, Finland.

Peltoniemi M.; 1998: *Depth of exploration of frequency-domain airborne electromagnetics in resistive terrains.* Explor. Geophys., **29**, 12-15.

Podgorski J.E., Kgotlhang L., Ngwisanyi T., Ploug C., Auken E., Kinzelbach W. and Green A.G.; 2010: *Introducing the Okavango Delta, Botswana, Airborne TEM Survey.* In: Proc. 16th, Eur. Meeting Environ. Eng. Geophys., Zurich, Switzerland, expanded abstracts, A19.

Reid J.E., Pfaffling A. and Vrbancich J.; 2006: *Airborne electromagnetic footprints in 1D earths.* Geophysics, **71**, G63-G72.

Sengpiel K.P. and Siemon B.; 2000: *Advanced inversion methods for airborne electromagnetic exploration*. Geophysics, **65**, 1983-1992.

Siemon B.; 2006: *Electromagnetic methods – frequency domain: Airborne techniques.* In: Kirsch R. (ed), Groundwater Geophysics – A Tool for Hydrogeology, Springer-Verlag, Berlin, Heidelberg, Germany, pp. 155-170.

Siemon B., Christiansen A.V. and Auken E.; 2009: *A review of helicopter-borne electromagnetic methods for groundwater exploration.* Near Surf. Geophys., **7**, 629-646.

Siemon B., Eberle D.G. and Binot F.; 2004: *Helicopter-borne electromagnetic investigation of coastal aquifers in North-West Germany.* Z. Geol. Wiss., **32**, 385-395.

Siemon B., Steuer A., Meyer U. and Rehli H.J.; 2007: *HELP ACEH - A post-tsunami helicopter-borne groundwater project along the coasts of Aceh, northern Sumatra.* Near Surf. Geophys., **5**, 231-240.

Smith R.S., Hodges G. and Lemieux; 2009: *Case histories illustrating the characteristics of the HeliGEOTEM system.* Explor. Geophys., **40**, 246-256.

Sorensen K.I. and Auken E.; 2004: *A new high-resolution helicopter transient electromagnetic system.* Explor. Geophys., **35**, 194-202.

Supper R., Motschka K., Ahl A., Bauer-Gottwein P., Gondwe B.R.N., Alonso G.M., Romer A., Ottowitz D. and Kinzelbach W.; 2009: *Spatial mapping of submerged cave systems by means of airborne electromagnetics: an emerging technology to support protection of endangered Karst aquifers.* Near Surf. Geophys., **7**, 613-627.

Thomsen R., Sondergaard V.H. and Sorensen K.I.; 2004: *Hydrogeological mapping as a basis for estabilishing site-specific groundwater protection zones in Denmark.* Hydrogeol. J., **12**, 550-562.

Viezzoli A., Auken E. and Munday T.; 2009: *Spatially constrained inversion for quasi 3D modelling of airborne electromagnetic data – an application for environmental assessment in the lower Murray Region of South Australia.* Explor. Geophys., **40**, 173-183.

Viezzoli A., Christiansen A.V., Auken E. and Sorensen K.I.; 2008: *Quasi-3D modeling of airborne TEM data by spatially constrained inversion.* Geophysics, **73**, F105-F113.

Viezzoli A., Tosi L., Teatini P. and Silvestri S.; 2010: *Surface water-groundwater exchange in transitional coastal envirnments by airborne electromagnetics: the Venice Lagoon example.* Geophys. Res. Lett., **37**, L01402.

Wiederhold H., Schaumann G. and Steuer A.; 2009: *Airborne geophysical investigations for hydrogeological purposes in northern Germany.* In: Proc. 15th Environ. and Eng. Geophys. Eur. Meeting - Near Surface, Dublin, Ireland, extended abstracts.

Witherly K., Irvine R. and Morrison E.B.; 2004: *The Geotech VTEM time-domain helicopter EM system.* In: Proc. 74th Annu. Int. Meeting Soc. Expl. Geophys., Denver, CO, USA, expanded abstracts, **23**, pp. 1217-1221.

Corresponding author: Andrea Viezzoli
Aarhus Geophysics
C.F. Møllers Allé 4, DK-8000 Aarhus C, Denmark
Phone: +39 3922979326; e-mail: andrea.viezzoli@aarhus-geo.com